Influence of nanoconfinement on structure and phase transitions in $RbNO_3$/porous glass composites

H. T. Nguyen [a,*], A. Yu. Milinskiy [b], S. V. Baryshnikov [b], I. A. Chernechkin [b], P. T. B. Thao [a]

[a] *Faculty of Electrical Engineering Technology, Industrial University of Ho Chi Minh City, Ho Chi Minh City, Vietnam*

[b] *Faculty of Physics and Mathematics, Blagoveshchensk State Pedagogical University, Blagoveshchensk, Russia*

This study aims at clarifying the structure, thermal and dielectric properties of a nanocomposite consisting of rubidium nitrate embedded in a porous borosilicate glass matrix (15.3 nm). Experimental data were obtained using X-ray diffraction, Fourier-transform infrared spectroscopy, differential thermal analysis and dielectric measurements, enabling the identification of the effects of nanoconfinement on the phase transitions. It was found that the temperature of phase transition from the trigonal to cubic phase in the filled rubidium nitrate was significantly reduced from 439 K to 422 K. This finding was corroborated by both differential thermal analysis, X-ray diffraction methods and Landau's phenomenological theory.

(Received June 7, 2025; Accepted August 15, 2025)

Keywords: Ferroelectrics nanocomposites, Rubidium nitrate, Porous borosilicate glass, Phase transition, Nanoconfinement

1. Introduction

One of the priority areas in modern materials science with high practical relevance is the physics of heterogeneous materials and systems [1, 2]. The growing interest in such structures arises from their ability to exhibit atypical properties that differ significantly from those of homogeneous ones. These unique characteristics stem from the complex interactions between distinct phases, which vary in chemical composition, crystal structure, and physico-chemical parameters. Additionally, interfacial boundaries make a significant contribution to the overall properties of the system, influencing transport, dielectric, and mechanical characteristics.

Composite materials, particularly ferroelectric composites composed of components with differing functional and structural parameters, are of particular interest. These composites typically consist of a ferroelectric matrix modified by inclusions of metallic, polymeric, or carbon-based nature. Such structural design enables the deliberate tuning of parameters such as dielectric permittivity, coercive field, phase transition temperature, and piezoelectric activity. As a result, these materials are highly attractive for a wide range of technological applications – from microelectronics to sensor systems and energy-saving technologies [3].

One of the promising directions in materials science is the use of borosilicate porous glasses as nanomatrices for the development of functional nanocomposites [4–6]. Filled porous glasses represent unique nanostructures in which the pore space is either partially or completely filled with various substances – ranging from simple compounds to chemically complex materials. The wide selection of possible fillers enables fine-tuning of the material's properties according to the specific application. For instance, numerous studies have investigated porous matrices filled with various ferroelectric compounds such as TGS, $NaNO_2$, $NaNO_3$, and KNO_3 [7–9]. The impregnation of a magnetic porous matrix with ferroelectric materials offers a route to the creation of multiferroic materials [10]. The structure and physical properties – particularly dielectric and

* Corresponding author: nguyenthuongfee@iuh.edu.vn
https://doi.org/10.15251/JOR.2025.214.505

magnetic properties – of porous matrices and glass-based nanocomposites are closely related to the characteristics of the original glasses.

Rubidium nitrate ($RbNO_3$) is known with a few applications in magneto hydrodynamic power generation and catalysis. $RbNO_3$ exhibits four thermodynamically stable crystalline phases over a wide temperature range – from room temperature up to its melting point (~ 587 K). At room temperature, $RbNO_3$ crystallizes in a trigonal symmetry corresponding to phase IV, which possesses spontaneous polarization with the formation of 180-degree domain structures that are characteristic for ferroelectrics [11]. This phase is stable up to approximately 437 K, where a transition to a paraelectric phase III occurs with a cubic structure. In a range of 437 – 492 K, $RbNO_3$ exists in this highly symmetric, non-polar phase [12]. Between 492 K and 558 K, transitions to a rhombohedral modification (phase II) are detected [13]. Upon further heating above 558 K, another phase transition takes place, reverting $RbNO_3$ to a cubic structure (phase I) which remains stable up to the melting point around 587 K.

The current applications of $RbNO_3$ have reached saturation, so a new approach is needed to control its inherent properties. In this regard, the present work is devoted to exploring anomalies of the structure, thermal and dielectric properties of nanocomposites based on $RbNO_3$ embedded in porous glass, aiming at expanding the applications of the current $RbNO_3$, as well as contributing to a deeper understanding of the processes in nanostructured systems.

2. Materials and methods

The procedures for materials preparation and the experimental measurements are briefly diagrammed in Figure 1. For the synthesis of the nanocomposite, $RbNO_3$ supplied by Sigma-Aldrich and porous borosilicate glasses with an average pore diameter of approximately 15.3 nm were used as starting materials. Incorporation of $RbNO_3$ into the porous glass was carried out by melt infiltration under a pressure of $2 \cdot 10^5$ Pa. The filling degree was determined gravimetrically based on the change in sample mass, using high-precision analytical balances (BM-252), and was found to be 72%, indicating a substantial volume of infiltrated material relative to the total pore volume. Pressed disks of $RbNO_3$ powder with a diameter of 10 mm and a thickness of 1.5 mm, obtained under a pressure of 8000 kg/cm², were used as reference samples.

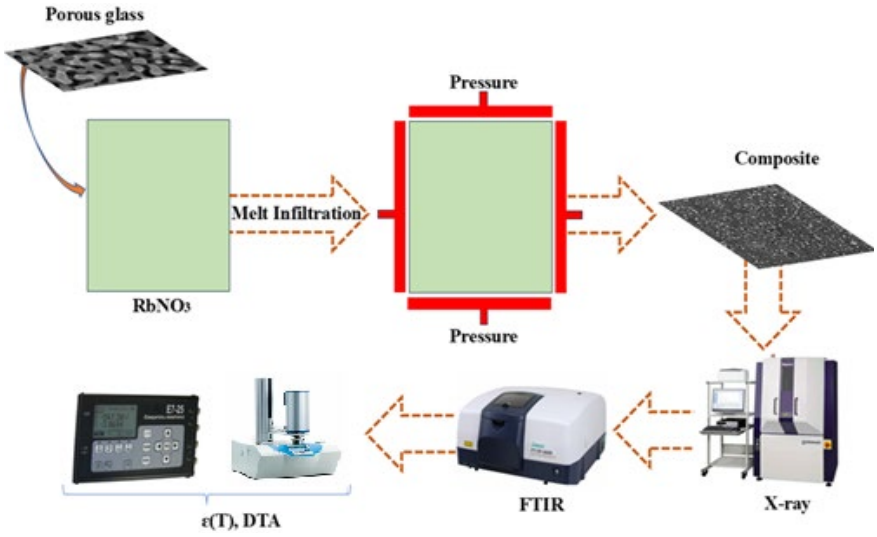

Fig. 1. Scheme for materials preparation and experimental measurements.

X-ray phase analysis of composite samples during heating and subsequent cooling was carried out using a Rigaku Ultima IV at temperatures selected at 300, 373, 413, 433, and 438 K,

allowing for the tracking of phase transitions. Functional groups were figured out by an IR spectrometer (IR 6000, Japan). Dielectric properties of the samples were conducted from 300 to 450 K using a digital impedance meter E7-25 with a heating rate of 1 K/min. Electrical contact was established using an indium-gallium paste. Temperature control was ensured by an electronic thermometer (TC-6621).

3. Experimental results

The temperature dependence of the dielectric permittivity *ε′(T)* was studied for polycrystalline $RbNO_3$ and the $RbNO_3$/porous glass nanocomposite (Figure 2). The phase transition in bulk $RbNO_3$ (determined from the maximum of the derivative of *ε′(T)*) was observed at 439 K during heating and at 436 K during cooling. For the nanocomposite, the curves *ε′(T)* did not show pronounced anomalies like those observed in the bulk (polycrystalline) samples. The absence of sharp peaks or jumps in *ε′(T)* indicates a smooth change in dielectric properties, which might be attributed to the inhomogeneity of the nanostructured medium, as well as the influence of interfacial boundaries and surface states that dominated in nanocomposites. Nevertheless, weak anomalies were observed at approximately 422 K during heating and around 393 K during cooling, which was likely related to the phase transitions.

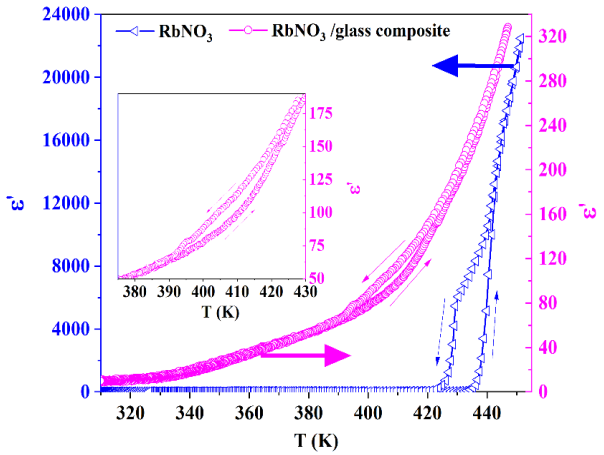

Fig. 2. Temperature dependencies of the dielectric permittivity ε′ for $RbNO_3$ (left axis) and $RbNO_3$ in porous glass (right axis). The inset shows the ε′(T) dependence in the temperature range of 375 – 430 K for porous glass filled with $RbNO_3$.

First-order phase transitions, characteristic of both bulk and nanostructured $RbNO_3$, were reliably recorded using differential thermal analysis (DTA) (Figure 3). For the bulk form, distinct endothermic and exothermic effects were observed at 437 K (during heating) and 423 K (during cooling), which were consistent with previously published data [11]. In the case of the nanocomposite, the phase transitions were shifted to lower temperatures. In the heating process, a DTA signal peak was observed at 422 K, while upon cooling - at approximately 391 K.

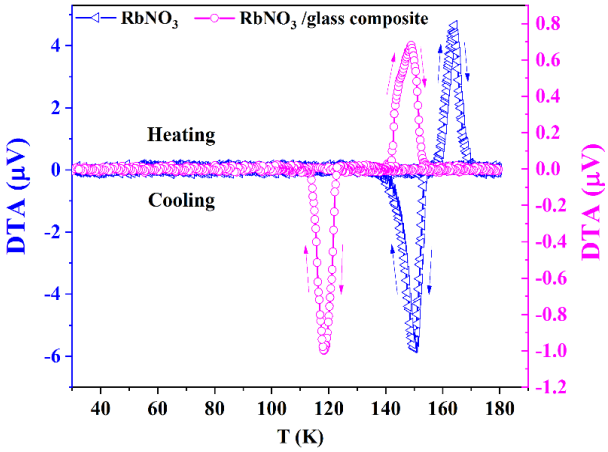

Fig. 3. Temperature dependencies of the DTA signal for $RbNO_3$ (left axis) and $RbNO_3$ in porous glass (right axis).

Regarding the adjustment of crystalline structure during phase transition, let us analyze the temperature – dependent XRD pattern of the composite (Figure 4). Obviously, except for the diffraction peaks of Cu (possibly, due to X-ray tube source (Cu Kα)) and Pt of sample holder, other peaks are characteristic for $RbNO_3$ according to reference data JCPDS 36-1257 (Figure 4a). For example, at 300 K (Table 1), the diffraction peaks of $RbNO_3$ correspond to the most prominent reflections identified at 2θ positions of 19.9°, 26.2°, 29.6°, 32.4°, 36.1°, 38.5°, 47.6°, 56.2°, 58.0°, 61.6°, 63.3°, and 72.7°, which are indexed to the (012), (104), (110), (024), (116), (202), (122), (214), (208), (300), (220), and (119) planes, respectively. These peaks confirm the presence of well-defined crystalline $RbNO_3$ within the nanocomposite. In addition to the $RbNO_3$ peaks, diffraction signals attributed to platinum (Pt) and copper (Cu) were also observed. The Pt reflections appear at 2θ values of 39.7°, 46.2°, 67.5°, and 81.2°, corresponding to the (111), (200), (220), and (311) planes. A single Cu peak is present at 43.3°, assigned to the (111) plane. These Pt and Cu peaks do not originate from the composite material itself but rather from the sample holder (Pt) and X-ray tube target (Cu), which are commonly encountered artifacts in XRD analysis. The main phase at 300 K is the trigonal modification of $RbNO_3$ with the space group P31, and lattice parameters a = 10.474 Å, c = 7.443 Å, V = 707.137 Å^3, which is consistent with the published data [14]. However, upon heating, there was the shift in peak positions detected with changes in peak shapes (Figure 4b).

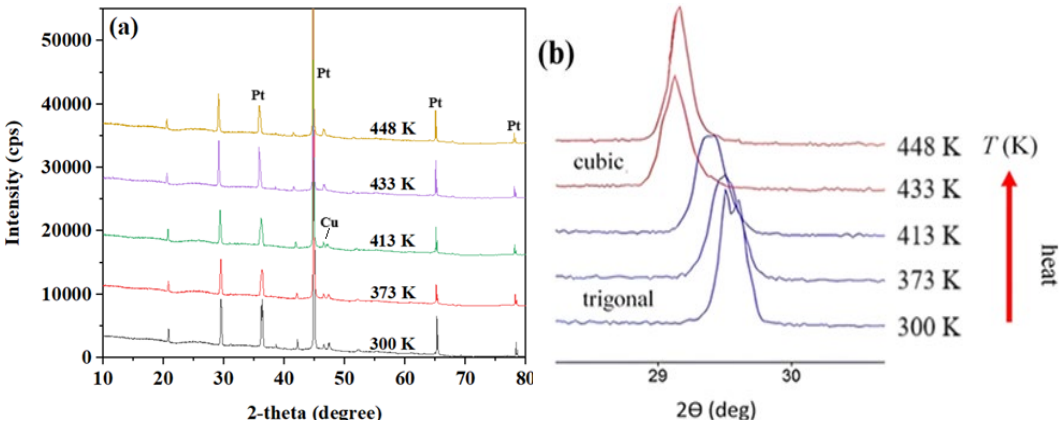

Fig. 4. Diffractogram for the $RbNO_3$/porous glass composite at different temperatures (a) and its fragment illustrating the phase transition region of rubidium nitrate (trigonal → cubic) between temperatures of 413 – 433 K (b).

This represents a polymorphic transition from the triclinic to the cubic modification in the temperature range of 413 – 433 K. The space group of the cubic phase at 438 K is Pm-3m, with parameters a = 4.37 Å and V = 83.45 Å^3. Regarding the borosilicate glass phase, it is an amorphous phase i.e. there is no sharp peaks appeared the XRD pattern.

Table 1. Interpretation of diffraction peaks obtained for $RbNO_3$/nanoporous glass composite at 300 K.

Phase	2θ Position (°)	Assigned Plane (hkl)
$RbNO_3$	19.9	(012)
	26.2	(104)
	29.6	(110)
	32.4	(024)
	36.1	(116)
	38.5	(202)
	47.6	(122)
	56.2	(214)
	58.0	(208)
	61.6	(300)
	63.3	(220)
	72.7	(119)
Pt	39.7	(111)
	46.2	(200)
	67.5	(220)
	81.2	(311)
Cu	43.3	(111)

The influence of nanoconfinement on the functional groups of $RbNO_3$ embedded in glass nanopores was also investigated. Comparing the IR spectra of $RbNO_3$ (Figure 5a) and the composite (Figure 5b) along with the absorption peaks exported from these spectra (Table 2) indicated a slight shift of the filled-$RbNO_3$ peaks positions. This might be attributed to the nanoconfinement effect and weak interactions between $RbNO_3$ and the pore surfaces. In other words, strong chemical bonding between $RbNO_3$ and the pores were absent and thus, these interactions did not influence the phase transitions. Consequently, under nanoconfinement, only a modification of the crystalline structure occurred, as confirmed above by the diffraction analysis.

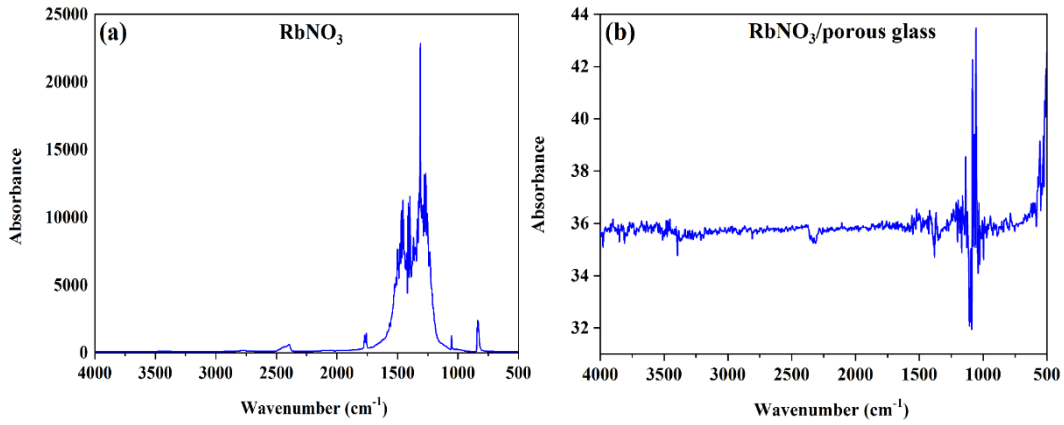

Fig. 5. FTIR spectra for $RbNO_3$ and $RbNO_3$ filled in porous glass.

Table 2. Peaks and functional groups exported from thr FTIR spectra for the bulk $RbNO_3$ (Fig. 5a) and $RbNO_3$/nanoporous glass composite (Fig. 5b).

Peaks positions	Bulk $RbNO_3$	$RbNO_3$/Borosilicate glass	Interpretation
1488 – 1417	Present	Present	Asymmetric stretching (ν_3) of NO_3^-
1386 – 1330	Present	Present	Symmetric stretching (ν_1) of NO_3^-
1284 – 1214	Present	Present	In-plane bending (ν_4) of NO_3^-
830 – 740	Present	Present	Out-of-plane bending (ν_2) of NO_3^-
1300 – 1000	Absent	Present	Si–O–Si asymmetric stretching (borosilicate network)
1100 – 950	Absent	Present	B–O vibrations (from BO_3 or BO_4 units of borosilicate glass)
3900 – 3300	Absent	Present	Broad –OH stretching vibrations
2314	Absent	Present	Weak CO_2 peak (likely from ambient contamination)

4. Theoretical models and discussions

When analyzing the temperature shifts of phase transitions in nanostructured systems with confined geometry, theoretical models that account for size effects are typically employed. The most widely used approaches are based on Landau's phenomenological theory and the Ising model, developed for individual isolated nanoparticles [15, 16]. These models predict that as the characteristic dimensions of the system decrease, the temperature of the structural phase transition should decrease and can be described as follows:

$$T_c(R) = T_c^{\infty} - \frac{A}{R} \tag{1}$$

where $T_c(R)$ and T_c^{∞} are the phase transition temperatures for a particle with radius R and the bulk material, respectively; A is a parameter depending on the material properties and the influence of surface effects. These predictions have been confirmed by many experimental studies on nanoparticles of ferroelectrics, such as barium titanate [17].

However, in the case of nanoparticles placed in a nanoporous matrix, additional factors related to specific interactions may influence the phase transition temperature, both with the internal surface of the porous structure and between nanoparticles localized in adjacent pores [18]. These effects can significantly modify the behavior of the system compared to isolated particles. For example, in the work [19], the increase in the temperature of the upper phase transition in ferroelectric nanoparticles synthesized inside porous Al_2O_3 was explained by the effect of polarization induced by the pore walls. According to Landau's phenomenological theory, this effect can be interpreted as an increase in the spontaneous polarization at the surface of the particles, which, in turn, contributes to the shift of the phase transition temperature to higher temperatures.

For a system containing $RbNO_3$ incorporated into porous glass, a different picture is observed. Apparently, the polarizability of the walls has a negligible effect on the behavior of the embedded particles. Instead, the observed decrease in the phase transition temperature might likely be related to the size effects observed for isolated nanoparticles with no significant interaction with the surrounding environment as proved by the above FTIR analysis. Let us calculate the decrease in phase transition temperature of $RbNO_3$ part. Firstly, the difference in thermal expansion coefficients between $RbNO_3$ and porous glass might lead to temperature-dependent elastic compressive or tensile deformations, which are expected to influence the phase transition temperature of the ferroelectric component. The thermal expansion coefficient of $RbNO_3$ is approximately 50×10^{-6} K^{-1} [20], whereas that of porous glass is about 5×10^{-6} K^{-1} [20]. The baric coefficient dT_c/dp of rubidium nitrate has been determined in [21] and is approximately 89 K/GPa.

To estimate the baric effect, we use the formula for calculating the hydrostatic pressure P [22] experienced by $RbNO_3$ particles located within the glass pores:

$$P = -\frac{E}{3(1-\mu)}\Delta\alpha\Delta T \quad (2)$$

where E is the Young's modulus, μ is the Poisson's ratio, $\Delta\alpha$ is the difference in the linear thermal expansion coefficients of the materials, and ΔT is the temperature difference between the stress-free and stressed states of the filler. The differences in E and μ of the contacting materials are neglected, as accounting for them would not significantly affect the order of magnitude of the effect. The calculated values of the defined quantities are listed in Table 3.

Table 3. Values of the quantities defined in Equation (2) for $RbNO_3$ in glass pores.

dT_c/dp, K/GPa	E, GPa	μ	$\Delta\alpha.10^6$, K^{-1}	ΔT, K	P, GPa	ΔT, K
89	15	0.25	60	200	-0.08	-7.12

As observed in Table 3, the baric coefficient of rubidium nitrate is positive. Therefore, in the case of tensile stress, an increase in hydrostatic pressure should result in a decrease in the phase transition temperature by an amount ΔT = 7.12 K. This indicates that, for $RbNO_3$ in porous glass, mechanical stress may be one of the factors contributing to the lowering of the phase transition temperature. These estimates are valid under the assumption of complete pore filling by rubidium nitrate and good adhesion between the materials. In our case, the pore-filling coefficient of rubidium nitrate is less than unity; hence, the reduction in the phase transition temperature due to the baric effect should be less than 7 K. Note that in a previously reported study [23], $RbNO_3$ embedded in porous Al_2O_3 films also showed a shift in the phase transition towards lower temperatures.

A particular scientific interest is the observed increase in the temperature hysteresis in the $RbNO_3$/porous glass nanocomposite system. For bulk ferroelectrics, a change in the nature (order) of the structural phase transition, or its deviation from the tricritical point, is usually associated with the influence of external pressure. In nanostructured composites containing $RbNO_3$ nanoparticles, the enhancement of first-order phase transition features can apparently be attributed to internal mechanical stresses that arise under the nanoconfienment conditions of the porous glass.

4. Conclusions

In summary, the incorporation of $RbNO_3$ into the confined space of nanoporous glass led to a significant reduction in the phase transition temperature, which was attributed to size effects. Differential thermal analysis data confirmed that temperature-dependent phase transitions in the nanocomposite occurred with more pronounced thermal hysteresis, which might indicate an enhancement of first-order phase transition features induced by internal mechanical stresses in the conditions of nanoconfinement. Exploring the structure of $RbNO_3$ embedded in porous glass during the phase transition has also demonstrated changes from the trigonal to the cubic phase without significant changes in the lattice parameters. Besides, the theoretical predictions based on Landau's phenomenological theory and the Ising model confirm the applicability of these models to describe the behavior of this type of nanostructured ferroelectrics. Thus, the use of porous glass as a nanomatrix for the creation of composites with $RbNO_3$ opens opportunities for targeted control of phase transitions and dielectric properties of the material, making such systems promising for the development of functional electronic components, sensors, and energy-active devices.

References

[1] V. N. Nechaev, A. V. Shuba, Physics of the Solid State **60**, 1332 (2018); https://doi.org/10.1134/S106378341807020X
[2] W. Chen, S. Yuan, Y. Ji, G.Jiang, J. Shao, Y. Zheng, MRS Advances **2**, 3427 (2017); https://doi.org/10.1557/adv.2017.316
[3] O. G. Vendik, M. A. Nikol'skii, Technical Physics **46**, 112 (2001); https://doi.org/10.1134/1.1340895
[4] E. Rysiakiewicz-Pasek, A. Ciżman, T. Antropova, Y. Gorokhovatsky, O. Pshenko, E. Fomicheva, I. Drozdova, Materials Chemistry and Physics **243**, 122585 (2020); https://doi.org/10.1016/j.matchemphys.2019.122585
[5] A. Y. Milinskiy, S. V. Baryshnikov, I. A. Chernechkin, Russian Physics Journal **65**, 1431 (2023); https://doi.org/10.1007/s11182-023-02787-6
[6] K. Idczak, E. Jach, D. A. Kowalska, P. Wieczorek, A. Ciżman, Applied Surface Science **669**, 160390 (2024); https://doi.org/10.1016/j.apsusc.2024.160390
[7] E. Rysiakiewicz-Pasek, J. Komar, A. Cizman, R. Poprawski, Journal of Non-Crystalline Solids **356**, 661 (2010); https://doi.org/10.1016/j.jnoncrysol.2009.07.035
[8] E. Koroleva, A. Naberezhnov, E. Rysiakiewicz-Pasek, R. Poprawski, Composites Part B: Engineering **94**, 322 (2016); https://doi.org/10.1016/j.compositesb.2016.03.046
[9] C. Tien, E. V. Charnaya, M. K. Lee, S. V. Baryshnikov, S. Y. Sun, D. Michel, W. Böhlmann, Physical Review B **72**, 104105 (2005); https://doi.org/10.1103/PhysRevB.72.104105
[10] A. Cizman, W. Bednarski, T. V. Antropova, O. Pshenko, E. Rysiakiewicz-Pasek, S. Waplak, R. Poprawski, Composites Part B: Engineering **64**, 16 (2014); https://doi.org/10.1016/j.compositesb.2014.03.024
[11] P. C. Bury, A. C. McLaren, physica status solidi (b) **31**, 799 (1969); https://doi.org/10.1002/pssb.19690310239
[12] P. P. Salhotra, E. C. Subbarao, P. Venkateswarlu, physica status solidi (b) **29**, 859 (1968); https://doi.org/10.1002/pssb.19680290238
[13] S. Fujimoto, N. Yasuda, H. Shimizu, S. Tsuboi, K Kawabe, Y. Takagi, M. Midorikawa, Journal of the Physical Society of Japan, **42**, 911 (1977); https://doi.org/10.1143/JPSJ.42.911
[14] M. Shamsuzzoha, B. W. Lucas, Acta Crystallographica Section B **B38**, 2353 (1982); https://doi.org/10.1107/S0567740882008772
[15] W. L. Zhong, Y. G Wang., P. L. Zhang, B. D. Qu, Physical Review B **50**, 698 (1994); https://doi.org/10.1103/PhysRevB.50.698
[16] C. L. Wang, Y. Xin, X. S. Wang, W. L. Zhong, Physical Review B **62**, 11423 (2000); https://doi.org/10.1080/00150190108016245
[17] P. Sedykh, D. Michel, Physical Review B **79**, 134119 (2009); https://doi.org/10.1103/PhysRevB.79.134119
[18] A. V. Uskov, E. V. Charnaya, A. L. Pirozerskii, A. S. Bugaev, Ferroelectrics **482**, 70 (2015); https://doi.org/10.1080/00150193.2015.1056708
[19] D. Yadlovker, S. Berger, Physical Review B **71**, 184112 (2005); https://doi.org/10.1103/PhysRevB.71.184112
[20] I. S. Grigoriev, E. Z. Meilikhov, A. A. Radzig (Eds.), "Handbook of Physical Quantities", CRC Press (Boca Raton, Florida, US), 1548 p. (1997)
[21] S. Fujimoto, N. Yasuda, H. Shimizu, S. Tsuboi, K. Kawabe, Y. Takagi, M. Midorikawa, Journal of the Physical Society of Japan **42**, 911 (1977). https://doi.org/10.1143/JPSJ.42.911
[22], O. M. Golitsyna, S. N. Drozhdin, V. N. Nechaev, A. V. Viskovatykh, V. M. Kashkarov, A. E. Gridnev, V. V. Chernyshev, Physics of the Solid State **55**, 529 (2013). https://doi.org/10.1134/S1063783413030128
[23] H. T. Nguyen, S. V. Baryshnikov, A. Yu. Milinsky, E. V. Stukova, Integrated Ferroeletrics **237**, 1 (2023); https://doi.org/10.1080/10584587.2023.2227052